

RESEARCH

Open Access



Concomitant aortic regurgitation predicts better left ventricular reverse remodeling after transcatheter aortic valve replacement

Hao-Ran Yang^{1†}, Tian-Yuan Xiong^{1†}, Yi Zhang¹, Jing-Jing He¹, Yuan Feng¹ and Mao Chen^{1*}

Abstract

Background We aim to determine predictors of inadequate left ventricular mass index (LVMI) regression at mid-term after transcatheter aortic valve replacement (TAVR), including the potential role of epicardial adipose tissue (EAT).

Methods We retrospectively reviewed patients with both echocardiographic assessments and multi-slice computed tomography (MSCT) obtained one year after TAVR. The change of LVMI, the volume and the average CT attenuation of EAT from baseline to one-year follow-up was calculated. Patients were divided into two groups by the percentage change of LVMI at a cut-off of 15%.

Results A total of 152 patients were included with a median age of 74 years (interquartile range [IQR] 69–78 years) and 56.6% being male. LVMI decreased ($P < 0.0001$) while EAT volume increased and the average CT attenuation decreased (both $P < 0.0001$) at one year. Baseline atrial fibrillation ($P = 0.042$), mitral regurgitation \geq mild ($P = 0.006$), aortic regurgitation (AR) $>$ mild ($P = 0.001$) and the change in the average CT attenuation of EAT ($P = 0.026$) were different between the decrease of LVMI $\geq 15\%$ and $< 15\%$. AR $>$ mild at baseline was the only statistically significant predictor of a decrease of LVMI $< 15\%$ at one year (OR 0.33, 95% CI: 0.13 to 0.84, $P = 0.021$) in multivariate regression.

Conclusions Concomitant more-than-mild AR might predict better left ventricular reverse remodeling regression after TAVR.

Keywords Transcatheter aortic valve replacement, Left ventricular reverse remodeling, Aortic regurgitation, Epicardial adipose tissue

Introduction

Left ventricular (LV) remodeling, which has been associated with worse clinical outcomes [1–4], is a common response to pressure overload caused by severe aortic stenosis (AS). The relief of this overload from transcatheter aortic valve replacement (TAVR) tends to provoke LV reverse remodeling, which is demonstrated as a decrease in left ventricular mass index (LVMI). In a previous study, it has been observed that LVMI underwent a rapid decrease in the first year after TAVR with a median percentage of decrease at 14.5% and reached a relative plateau afterwards. [5]. The degree of LVMI

[†]These two authors contributed equally to the work.

*Correspondence:

Mao Chen
maochen@pcrccv.com

¹Department of Cardiology and Laboratory of Heart Valve Disease, West China Hospital, Sichuan University, #37 Guoxue Alley, Chengdu 610041, PR China



regression varies across patients and it could serve as an independent predictor of postoperative outcomes after TAVR in patients without significant paravalvular leakage (PVL) [6]. Given its impact on the prognosis, it is of great importance to ascertain the predictors of LVMI regression after TAVR. Previous studies have identified that male and TAVR-induced left bundle branch block (LBBB) predict less favorable LV reverse remodeling [7, 8]. Besides, it is noteworthy that some studies have found the volume of epicardial adipose tissue (EAT) is associated with LV remodeling in the progression of calcific AS and the clinical outcomes after TAVR [9–11]. However, the change in the volume and the average CT attenuation of EAT after TAVR and their relationship with LV reverse remodeling remain unclear. Herein, we retrospectively reviewed TAVR patients in our center and compared two groups of patients by the degree of LVMI regression at one year, with the aim of determining predictors of inadequate LVMI regression.

Methods

Patient population

We retrospectively included patients with severe symptomatic AS who underwent TAVR in our center with both echocardiographic assessments and multi-slice computed tomography (MSCT) obtained one year after TAVR. Patients with failed aortic bioprostheses were excluded. The indication for TAVR was discussed in all cases by our multidisciplinary Heart Team. Baseline and clinical characteristics, echocardiographic and computed tomographic measurements, as well as procedural and post-procedural details were collected in a dedicated prospective TAVR database. This study was approved by the institutional review board and all patients gave written informed consent.

Procedures

All of the procedures were performed under general anesthesia in the hybrid operating room before September 2016 and in the catheterization laboratory with local anesthesia and conscious sedation afterwards. The transfemoral approach was the default choice of access. Balloon pre- and post-dilation were performed according to operator discretion. Transcatheter heart valves used during the study period were mainly domestic first generation self-expanding devices with no outer skirt or recapturable capability (i.e. Venus-A valve, Venus MedTech, Inc., Hangzhou, China; VitaFlow valve, MicroPort, Shanghai, China). The size of transcatheter heart valve was determined according to the comprehensive analysis of annular dimension and landing zone calcification. A second valve might need to be implanted in the index procedure due to valve migration or significant PVL.

Echocardiography

Transthoracic echocardiography (TTE) was arranged at baseline and at follow-ups after TAVR. The severity of aortic regurgitation (AR) and mitral regurgitation (MR) was determined by two experienced echocardiographers. The main grading criteria for AR were vena contracta width (CVW) and/or the ratio of the width of AR jet to the diameter of the left ventricular out flow tract, where the $CVW < 0.3$ cm and/or the ratio $< 25\%$ indicated mild AR, $0.3 \text{ cm} \leq CVW \leq 0.6$ cm and/or $25\% \leq$ the ratio $< 65\%$ indicated the moderate AR, $CVW > 0.6$ cm and/or the ratio $\geq 65\%$ indicated severe AR [12]. The main criterion for MR was the CVW, where $CVW < 0.3$ cm indicated mild MR while $CVW \geq 0.7$ cm indicated severe MR. [12] When grading severity was difficult by the parameters mentioned above, other qualitative or quantitative parameters were used according to the guidelines [12]. Left ventricular inner diameter in diastole (LVIDd), intra-ventricular septum in diastole (IVSd), and LV posterior wall in diastole (LVPWd) were measured in parasternal long axis view in accordance with guidelines recommendations [13]. LVM was calculated by the formula $LVM = 0.8 \times 1.04 \times ([LVIDd + IVSd + LVPWd]^3 - LVIDd^3) + 0.6$ g and divided by body surface area to acquire LVMI. Patients were divided into two groups by the percentage change of LVMI (i.e. $[\text{baseline LVMI} - 1\text{-year LVMI}] / \text{baseline LVMI}$) at a cut-off of 15% according to the observation that the median percentage decrease of LVMI was 14.5% at one year [5].

MSCT protocol and measurements

Pre-procedural MSCT was done for procedural planning while post-procedural MSCT was done to monitor structural valve deterioration. All MSCT scans were contrasted and performed with a second-generation dual-source CT system (SIEMENS SOMATOM Definition Flash; SIEMENS Healthcare, Erlangen, Germany). EAT volume and the average attenuation were semi-automatically quantified on MSCT using a commercially available software, Horos software ver. 2.0.2 (Horos Project, Annapolis, MD, USA). For each CT image, several contours were manually created to trace pericardial borders on axial images started at the level of the pulmonary trunk and ended at the level of the inferior diaphragmatic surface of the heart. The software then automatically generated missing borders that can be manually adjusted. The area outside the traced pericardium was excluded. The range of attenuation for EAT segmentation was then set between -10 and -190 HU [14], which allowed the exclusion of other tissues in the region of interest (Fig. 1). Total EAT volume was automatically obtained by multiplying the sum of all measured areas by the slice thickness and the overall average CT attenuation was calculated as

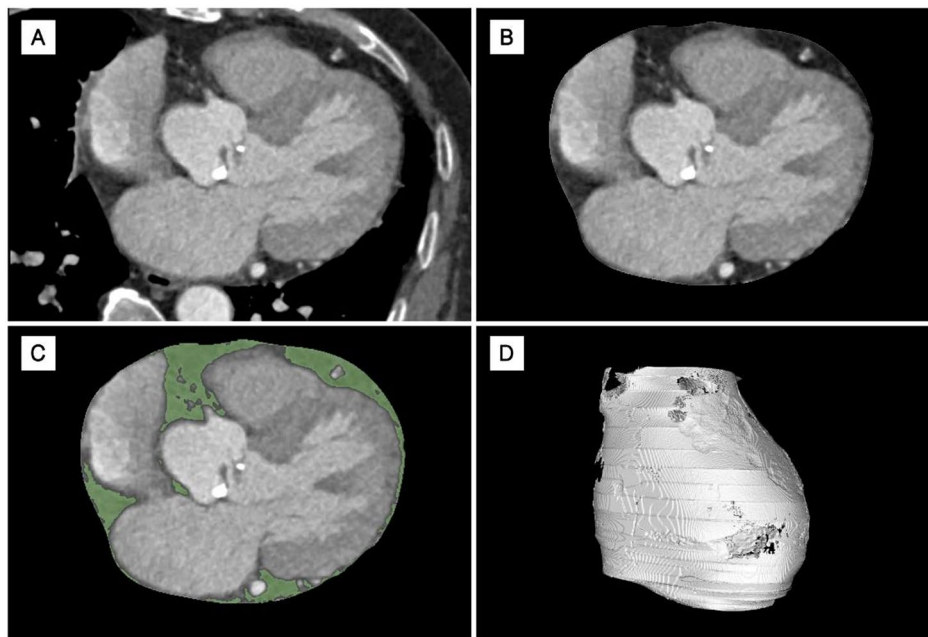


Fig. 1 Measurement of EAT on CT imaging. Panel (A) manual contour of the pericardial border; Panel (B) automatic exclusion of structures outside the contour by the software; Panel (C) identification of the range of attenuation between -10 and -190 HU automatically by the software; Panel (D) The 3D reconstruction of the EAT layer and its volume was automatically obtained by multiplying the sum of all measured areas by the slice thickness

the mean of all EAT voxels' attenuation automatically by the software.

Statistics

Continuous variables are presented as mean \pm standard deviation or median (interquartile range, IQR). Categorical variables were presented as frequencies and percentages. Comparisons were performed in baseline and clinical characteristics, echocardiographic and computed tomographic measurements, as well as procedural and post-procedural details between the two groups divided by LVMI change. Differences in proportions were assessed using the Chi-squared test or Fisher's exact test while differences in means between groups with continuous variables were assessed using an unpaired Student's *t* test; or when the variables were not normally distributed, Mann-Whitney non-parametric test was used to test ranks. If statistically significant, a multivariate logistic regression with variables that were different between groups was then performed adjusted by age and sex. The sufficiency of data had been taken into consideration and Hosmer-Lemeshow test was used to assess the model's goodness-of-fit. All computations relied on a commercially available software, SPSS version 21.0 software (IBM, Chicago, Illinois, USA), with statistical significance set at two-tailed 0.05.

Results

A total of 152 patients were included. The median age of these patients was 74 years (IQR 69–78 years), and male ($n=86$) accounted for 56.6%. LVMI decreased (163.7 [IQR:133.9-194.3] g/m^2 vs. 119.2 [IQR:102.3-144.6] g/m^2 , $P<0.0001$) significantly one year post-TAVR, but 28.9% of patients had inadequate LVMI regression (17.8% of patients had a decrease less than 15% while 11.2% of patients had an increase of LVMI). The median EAT volume at baseline was 108.0 cm^3 (IQR 85.9 - 139.4 cm^3) and 112 patients had an increase in EAT volume at one-year follow-up with a median Δ EAT volume (i.e. 1-year EAT volume – baseline EAT volume) of 16.7 cm^3 (IQR -0.7 – 24.9 cm^3). Meanwhile, the average CT attenuation of EAT at baseline was -63.07 ± 9.66 HU and 119 patients had an decrease in average CT attenuation of EAT at one-year follow-up with a mean Δ EAT attenuation (i.e. average CT attenuation of EAT at 1-year follow-up – average CT attenuation of EAT at baseline) of -7.46 HU (95% CI: -8.97 to -5.96 HU).

Between groups of adequate (i.e. a decrease of $\text{LVMI} \geq 15\%$) and inadequate (i.e. a decrease of $\text{LVMI} < 15\%$) LV reverse remodeling, baseline atrial fibrillation (10.2% vs. 22.7%, $P=0.042$), mitral regurgitation \geq mild (63.0% vs. 38.6%, $P=0.006$), aortic regurgitation (AR) $>$ mild (43.5% vs. 15.9%, $P=0.001$) as well as Δ EAT attenuation (-8.40 ± 10.08 HU vs. -5.16 ± 6.93 HU, $P=0.026$) were statistically different (Table 1). In the multivariate regression adjusted by age and sex

Table 1 Difference between groups in baseline characteristics, procedural details and echocardiographic data

	Adequate LVMI regression N = 108	Inadequate LVMI regression N = 44	P value
Baseline characteristics			
Age (year)	74 (68–78)	74 (70–80)	0.138
Male, n (%)	62 (57.4)	24 (54.5)	0.747
Height (cm)	1.60 (1.53–1.68)	1.60 (1.55–1.68)	0.658
Weight (kg)	57.6 ± 9.5	58.0 ± 8.5	0.816
BMI (kg/m ²)	22.6 ± 3.4	22.4 ± 3.0	0.831
BSA (m ²)	1.68 ± 0.15	1.69 ± 0.14	0.680
STS Score (%)	6.82 (4.19–9.25)	5.82 (4.04–8.51)	0.320
NYHA class III–IV, n (%)	97 (89.8)	39 (88.6)	0.939
Hypertension, n (%)	41 (38.0)	18 (40.9)	0.735
Diabetes, n (%)	18 (16.7)	11 (25.0)	0.236
COPD, n (%)	64 (59.3)	23 (52.3)	0.430
AF, n (%)	11 (10.2)	10 (22.7)	0.042
CAD, n (%)	36 (33.33)	17 (38.64)	0.534
Previous PCI, n (%)	9 (8.3)	4 (9.1)	0.866
Previous MI, n (%)	2 (1.9)	0 (0.0)	0.999
CVD, n (%)	21 (19.4)	13 (29.6)	0.175
eGFR (ml/min/1.73m ²)	49.6 (38.0–65.2)	51.7 (40.9–61.5)	0.521
Echocardiography			
MS ≥ mild, n (%)	7 (6.5)	3 (6.8)	0.776
MR ≥ mild, n (%)	68 (63.0)	17 (38.6)	0.006
AR > mild, n (%)	48 (44.4)	7 (15.9)	0.001
LVEF (%)	58.0 (43.0–68.0)	62.5 (55.0–70.5)	0.064
Mean PG (baseline, mmHg)	63.0 (51.0–82.0)	57.0 (47.0–71.8)	0.132
Mean PG (1-year post-TAVR, mmHg)	11.0 (8.0–15.0)	11.0 (8.0–15.8)	0.847
MSCT			
Bicuspid valve, n (%)	56 (51.9)	29 (65.9)	0.113
Annulus perimeter (cm)	78.8 (72.6–84.0)	73.6 (70.6–84.3)	0.193
LVOT perimeter (cm)	81.2 (73.3–91.5)	77.2 (70.4–86.3)	0.105
STJ perimeter (cm)	95.8 (87.8–105.8)	93.80 (88.7–104.2)	0.563
SOV perimeter (cm)	109.6 (101.8–118.5)	110.4 (98.6–117.2)	0.517
EAT volume (Baseline, cm ³)	107.3 (77.0–141.6)	109.4 (91.0–137.5)	0.536
EAT volume (1-year post-TAVR, cm ³)	133.2 ± 54.5	127.3 ± 43.8	0.591
ΔEAT volume (cm ³)	19.0 (1.0–34.2)	10.1 (-5.0–23.4)	0.092
EAT attenuation (Baseline, HU)	-62.36 ± 9.84	-64.96 ± 9.12	0.138
EAT attenuation (1-year post-TAVR, HU)	-70.76 ± 8.37	-70.12 ± 8.36	0.669
ΔEAT attenuation (HU)	-8.40 ± 10.08	-5.16 ± 6.93	0.026
Procedural details			
Pre-dilation, n (%)	98 (90.7)	39 (88.6)	0.923
Post-dilation, n (%)	50 (46.3)	22 (50.0)	0.678
s valve implantation, n (%)	11 (10.2)	4 (9.1)	0.925
Post-procedural outcomes			
PVL ≥ mild, n (%)	33 (30.6)	9 (20.5)	0.207
New LBBB, n (%)	32 (29.6)	16 (36.4)	0.418
PPI, n (%)	23 (21.3)	13 (29.6)	0.278

Values are mean ± SD, n (%), or median (interquartile range). BMI = body mass index; BSA = body surface area; STS = Society of Thoracic Surgeons; NYHA = New York Heart Association; COPD = chronic obstructive pulmonary disease; AF = atrial fibrillation; CAD = coronary artery disease; PCI = percutaneous coronary intervention; MI = myocardial infarction; CVD = cerebrovascular disease; eGFR = evaluated glomerular filtration rate; MS = mitral stenosis; MR = mitral regurgitation; AR = aortic regurgitation; LVEF = left ventricular ejection fraction; PG = pressure gradient of aortic valve; LVOT = left ventricular outflow tract; STJ = sinotubular junction; SOV perimeter = perimeter sinus of Valsalva; EAT = epicardial adipose tissue; ΔEAT volume = EAT volume (1-year follow-up) - EAT volume (Baseline); PVL = perivalvular leakage; LBBB = left bundle branch block; PPI = permanent pacemaker implantation

(Table 2), more than mild AR at baseline remained as the only statistically significant predictor of the decrease of LVMi < 15% at one year (OR 0.33, 95% CI: 0.13 to 0.84, P=0.021). Hosmer-Lemeshow test showed a satisfying goodness-of-fit of this model (P=0.378).

Discussion

The main findings of our study are that (1) LVMi underwent a more pronounced decrease at one year when AS is concomitant with more than mild AR at baseline in TAVR recipients. (2) EAT, being recognized to exert endocrine and paracrine effects [15], also had a dynamic change post-TAVR.

It is known that isolated AS exerts only pressure overload to the LV myocardium while AS concomitant with AR exerts both pressure and volume overload. This different pathologic adaptation might lead to different structural changes of LV following treatment. In a previous study, *E. Mara Vollema et al.* found the decrease in LVMi was more pronounced in patients with isolated AR during the first year after surgical AVR than isolated AS [16]. Thus, we assumed that the different pattern of LV remodeling caused by coexisting AR contributes to, at least partly, a different time course of LV reverse remodeling in TAVR recipients. Moreover, from an outcome perspective, *Johnny Chahine et al.* have reported a better overall survival in patients with AS accompanied by AR compared to patients with isolated AS [17]. It is likely that the different response of LV reverse remodeling from TAVR might be a possible contributor to this survival benefit brought by coexisting AR as a more pronounced decrease in LVMi has been associated with better prognosis [5, 18]. Although PVL can also exert volume overload to the LV myocardium, it differs from AR at baseline as it is a remaining or newly emerged hemodynamic change after TAVR in the absence of AS. Post-TAVR PVL in this cohort, however, did not result in different LVMi. There might be two possible explanations. It is noteworthy that we conducted statistical analyses of PVL that was mild and above (mild in 33 cases and mild-to-moderate in 9 cases) while only more than mild AR was included in statistical analyses (mild-to-moderate in 14 cases and moderate or above in 41 cases). The reason that we

include mild PVL in the PVL group is that it is now recognized that even mild PVL affects outcomes after TAVR [19]. Therefore, it is obvious that the regurgitant volume of PVL cases was much smaller than cases with AR at baseline. Besides, the duration of volume overload caused by PVL was much shorter than hemodynamic disorders caused by AR at baseline as well.

In addition, our analysis adds the little evidence existed for the dynamic change of EAT post-TAVR. We observed an overall increase in EAT volume and an overall decrease in the average CT attenuation of EAT during 1-year follow-up from CT imaging post-TAVR, although these changes failed to be correlated with clinical outcomes. It has been shown that there is no anatomical barrier between EAT and the adjacent heart structures [20], which allows crosstalk between the two. EAT can exhibit either protective or harmful property for the underlying myocardium in different circumstances [21], and therefore, it has been suggested to play a part in several heart diseases. In heart failure, EAT is involved in the development and progression of disease through several mechanisms including increased inflammation and fibrosis, autonomic dysregulation and mechanic effects [22]. A strong correlation has been demonstrated between an increased EAT volume and worsening left ventricular diastolic relaxation and filling [23, 24]. A larger EAT volume at baseline has been previously associated with a worse prognosis after TAVR (an increased all-cause 1-, 2-, and 3-year mortality and an increased risk to reach the early safety endpoint) [11], although the study did not monitor volumetric changes of EAT during follow-up. Besides volume, CT attenuation might also be an important parameter of EAT, given that CT attenuation of EAT is determined by the adipocyte size/adipose tissue lipid content and interstitial fibrosis [22, 25]. In coronary artery disease, fat attenuation index (FAI), which is defined as the average attenuation of adipose tissue within a volume of interest as measured from reconstructed CT, was first proposed by *Alexios S. Antonopoulos et al.* as a marker of perivascular adipose tissue (PVAT) inflammation [25]. In their research, the differentiation of preadipocytes and intracellular lipid accumulation were found to be restrained by the

Table 2 Multivariate regression for inadequate LV reverse remodeling post-TAVR

	Univariate analysis		Multivariate analysis	
	OR (95% CI)	P value	OR (95% CI)	P value
Age (years)	1.05(0.99–1.11)	0.084	1.04(0.97–1.10)	0.269
Sex (male)	0.89(0.44–1.80)	0.747	0.94(0.43–2.06)	0.878
AF	2.60(1.01–6.65)	0.047	2.22(0.81–6.11)	0.123
MR (≥ mild)	0.37(0.18–0.76)	0.007	0.55(0.25–1.21)	0.138
AR (>mild)	0.24(0.10–0.58)	0.002	0.33(0.13–0.84)	0.021
ΔEAT attenuation (HU)	1.04(0.99–1.08)	0.058	1.02(0.97–1.06)	0.433

CI=confidence interval; OR=odds ratio; other abbreviations as in Table 1

contiguous vascular inflammation, which could be visualized as an increase in the attenuation of corresponding PVAT on CT imaging [25]. Therefore, FAI could be used to detect vascular inflammation and discriminate stable and unstable coronary plaques. The perivascular FAI has been translated into clinical practice for its ability to predict and stratify cardiac risk and a high perivascular FAI value (cutoff ≥ 70.1 HU) has been found as an indicator of increased cardiac mortality [26]. The decrease in the average CT attenuation observed in our research might also suggest a shift in the property of EAT. However, FAI is a relatively precise measurement to evaluate adipose tissues surrounding the vessel within millimeters but we only measured a rough average attenuation of the whole EAT surrounding the heart. The fact that this rough value decreased following TAVR merits further identification of regional property indicators of EAT besides its overall volume change. Neither the change in volume nor in CT attenuation of EAT was found to affect clinical outcomes in the current analysis. It is possible that at one year post-TAVR, the relief of pressure overload remains the main player that impacts LV reverse remodeling and the effect of EAT changes on LV myocardium might emerge afterwards, thus longer follow-up is warranted to understand the corresponding consequences.

Our results have limitations inherent to single-center retrospective studies, including a small sample size, selection and treatment bias, and the absence of blinded core-laboratory adjudicated echocardiographic and MSCT measurements. There could be a survival bias because the data in this study are collected from patients who completed one-year echocardiographic and MSCT follow-ups.

Conclusion

Patients underwent TAVR with pre-existing > mild AR appeared to experience a more pronounced LV reverse remodeling at mid-term.

Abbreviations

AF	atrial fibrillation
AR	aortic regurgitation
AS	aortic stenosis
BMI	body mass index
BSA	body surface area
CAD	coronary artery disease
CI	confidence interval
COPD	chronic obstructive pulmonary disease
CVW	vena contracta width
EAT	epicardial adipose tissue
eGFR	evaluated glomerular filtration rate
FAI	fat attenuation index
IQR	interquartile range
IVSd	intraventricular septum in diastole
LBbB	left bundle branch block
LV	left ventricular
LVIDd	left ventricular inner diameter in diastole
LVMi	left ventricular mass index
LVOT	left ventricular outflow tract

LVPWd	left ventricular posterior wall in diastole
MI	myocardial infarction
MR	mitral regurgitation
MS	mitral stenosis
MSCT	multi-slice computed tomography
NYHA	New York Heart Association
OR	odds ratio
PCI	percutaneous coronary intervention
PG	pressure gradient of aortic valve
PPI	permanent pacemaker implantation
PVL	paravalvular leakage
PVAT	perivascular adipose tissue
SOV	sinus of Valsalva
STJ	sinutubular junction
STS	Society of Thoracic Surgeons
TAVR	transcatheter aortic valve replacement
TTE	Transthoracic echocardiography

Acknowledgements

Not applicable.

Authors' contributions

Hao-Ran Yang, Tian-Yuan Xiong, Mao Chen and Yuan Feng wrote the main manuscript text while Yi Zhang and Jing-Jing He prepared the figure and tables. All authors reviewed the manuscript.

Funding

This work was supported by the National Natural Science Foundation of China (82102129, 82170375 and 81970325); Key Research and Development Project of Science & Technology Department of Sichuan Province (2022ZDZX0020); Sichuan Science and Technology Program (2022ZDZX0030); Key Research and Development Support Project of Science & Technology Department of Chengdu (2021-YF08-00121-GX); Chinese Medical Association Cardiovascular Branch (CSC) Clinical Research Special Fund Project (CSCF2020B04); West China Hospital "1.3.5" Discipline of Excellence Project- "Mechanisms of aortic stenosis and the clinical applications".

Data availability

The datasets used and/or analyzed during the current study are available from the corresponding author on reasonable request.

Declarations

Ethics approval and consent to participate

This study was approved by the institutional review board (Clinical Trial Ethics Committee of West China Hospital) and all patients gave written informed consent. All methods were carried out in accordance with relevant guidelines and regulations (Declaration of Helsinki).

Consent for publication

Not applicable.

Competing interests

The authors declare no competing interests.

Received: 11 April 2023 / Accepted: 2 July 2023

Published online: 17 July 2023

References

1. Burchfield JS, Xie M, Hill JA. Pathological ventricular remodeling: mechanisms: part 1 of 2. *Circulation*. 2013;128:388–400.
2. Cioffi G, Faggiano P, Vizzardi E, et al. Prognostic effect of inappropriately high left ventricular mass in asymptomatic severe aortic stenosis. *Heart*. 2011;97:301–7.
3. Levy D, Garrison RJ, Savage DD, Kannel WB, Castelli WP. Prognostic implications of echocardiographically determined left ventricular mass in the Framingham Heart Study. *N Engl J Med*. 1990;322:1561–6.

4. Mihaljevic T, Nowicki ER, Rajeswaran J, et al. Survival after valve replacement for aortic stenosis: implications for decision making. *J Thorac Cardiovasc Surg*. 2008;135:1270–8. discussion 8–9.
5. Chau KH, Douglas PS, Pibarot P, et al. Regression of Left Ventricular Mass after Transcatheter aortic valve replacement: the PARTNER trials and registries. *J Am Coll Cardiol*. 2020;75:2446–58.
6. Oh JK, Lee SH, Lee SA, et al. Prognostic impact of left ventricular mass regression after transcatheter aortic valve replacement in patients with left ventricular hypertrophy. *Int J Cardiol*. 2021;332:60–6.
7. Chen SC, Leu HB, Chang HH, et al. Women had favourable reverse left ventricle remodelling after TAVR. *Eur J Clin Invest*. 2020;50:e13183.
8. Dobson LE, Musa TA, Uddin A, et al. The impact of trans-catheter aortic valve replacement induced left-bundle branch block on cardiac reverse remodeling. *J Cardiovasc Magn Reson*. 2017;19:22.
9. Arangalage D, Mathieu T, Nguyen V, et al. Epicardial adipose tissue volume is associated with left ventricular remodeling in calcific aortic valve stenosis. *Arch Cardiovasc Dis*. 2019;112:594–603.
10. Davin L, Nchimi A, Ilardi F, et al. Epicardial adipose tissue and myocardial fibrosis in aortic stenosis relationship with symptoms and outcomes: a study using Cardiac magnetic resonance imaging. *JACC Cardiovasc Imaging*. 2019;12:213–4.
11. Eberhard M, Stocker D, Meyer M, et al. Epicardial adipose tissue volume is associated with adverse outcomes after transcatheter aortic valve replacement. *Int J Cardiol*. 2019;286:29–35.
12. Zoghbi WA, Adams D, Bonow RO, et al. Recommendations for noninvasive evaluation of native valvular regurgitation: a report from the American Society of Echocardiography developed in collaboration with the Society for Cardiovascular magnetic resonance. *J Am Soc Echocardiogr*. 2017;30:303–71.
13. Lang RM, Badano LP, Mor-Avi V, et al. Recommendations for cardiac chamber quantification by echocardiography in adults: an update from the American Society of Echocardiography and the European Association of Cardiovascular Imaging. *J Am Soc Echocardiogr*. 2015;28:1–39. e14.
14. Nappi C, Ponsiglione A, Acampa W, et al. Relationship between epicardial adipose tissue and coronary vascular function in patients with suspected coronary artery disease and normal myocardial perfusion imaging. *Eur Heart J Cardiovasc Imaging*. 2019;20:1379–87.
15. Madonna R, Massaro M, Scoditti E, Pescetelli I, De Caterina R. The epicardial adipose tissue and the coronary arteries: dangerous liaisons. *Cardiovasc Res*. 2019;115:1013–25.
16. Vollema EM, Singh GK, Pihadi EA, et al. Time course of left ventricular remodeling and mechanics after aortic valve surgery: aortic stenosis vs. aortic regurgitation. *Eur Heart J Cardiovasc Imaging*. 2019;20:1105–11.
17. Chahine J, Kadri AN, Gajulapalli RD, et al. Outcomes of transcatheter aortic valve replacement in mixed aortic valve disease. *JACC Cardiovasc Interv*. 2019;12:2299–306.
18. Lindman BR, Stewart WJ, Pibarot P, et al. Early regression of severe left ventricular hypertrophy after transcatheter aortic valve replacement is associated with decreased hospitalizations. *JACC Cardiovasc Interv*. 2014;7:662–73.
19. Schoechlin S, Hein M, Brennemann T, et al. 5-Year outcomes after transcatheter aortic valve implantation: focus on paravalvular leakage assessed by echocardiography and hemodynamic parameters. *Catheter Cardiovasc Interv*. 2022;99:1582–9.
20. Iacobellis G, Corradi D, Sharma AM. Epicardial adipose tissue: anatomic, biomolecular and clinical relationships with the heart. *Nat Clin Pract Cardiovasc Med*. 2005;2:536–43.
21. Iacobellis G. Local and systemic effects of the multifaceted epicardial adipose tissue depot. *Nat Rev Endocrinol*. 2015;11:363–71.
22. Iacobellis G. Epicardial adipose tissue in contemporary cardiology. *Nat Rev Cardiol*. 2022;19:593–606.
23. Doesch C, Haghi D, Fluchter S, et al. Epicardial adipose tissue in patients with heart failure. *J Cardiovasc Magn Reson*. 2010;12:40.
24. Doesch C, Streitner F, Bellm S, et al. Epicardial adipose tissue assessed by cardiac magnetic resonance imaging in patients with heart failure due to dilated cardiomyopathy. *Obes (Silver Spring)*. 2013;21:E253–61.
25. Antonopoulos AS, Sanna F, Sabharwal N, et al. Detecting human coronary inflammation by imaging perivascular fat. *Sci Transl Med* 2017;9.
26. Oikonomou EK, Marwan M, Desai MY, et al. Non-invasive detection of coronary inflammation using computed tomography and prediction of residual cardiovascular risk (the CRISP CT study): a post-hoc analysis of prospective outcome data. *Lancet*. 2018;392:929–39.

Publisher's note

Springer Nature remains neutral with regard to jurisdictional claims in published maps and institutional affiliations.